Am J Physiol Renal Physiol 285: F1168–F1178, 2003.
First published July 29, 2003; 10.1152/ajprenal.00171.2003.

The isolated polycystin-1 cytoplasmic COOH terminus prolongs ATP-stimulated Cl^- conductance through increased Ca^{2+} entry

Scott S. Wildman,[1,2,3] Kimberly M. Hooper,[1] Clare M. Turner,[2,3] James S. K. Sham,[4] Edward G. Lakatta,[5] Brian F. King,[3] Robert J. Unwin,[2,3] and Michael Sutters[1]

[5]*Laboratory of Cardiological Sciences, Gerontology Research Center, Division of* [1]*Renal Medicine, Johns Hopkins Bayview Medical Center, and* [4]*Division of Pulmonary and Critical Care Medicine, Johns Hopkins University, Baltimore, Maryland 21224; and* [2]*Center for Nephrology and* [3]*Department of Physiology/Autonomic Neuroscience Institute, Royal Free and University College Medical School, University College London, London, W1T 3AA United Kingdom*

Submitted 1 May 2003; accepted in final form 28 July 2003

Wildman, Scott S., Kimberly M. Hooper, Clare M. Turner, James S. K. Sham, Edward G. Lakatta, Brian F. King, Robert J. Unwin, and Michael Sutters. The isolated polycystin-1 cytoplasmic COOH terminus prolongs ATP-stimulated Cl^- conductance through increased Ca^{2+} entry. *Am J Physiol Renal Physiol* 285: F1168–F1178, 2003. First published July 29, 2003; 10.1152/ajprenal.00171.2003.—The precise steps leading from mutation of the polycystic kidney disease (*PKD1*) gene to the autosomal dominant polycystic kidney disease (ADPKD) phenotype remain to be established. Fluid accumulation is a requirement for cyst expansion in ADPKD, suggesting that abnormal fluid secretion into the cyst lumen might play a role in disease. In this study, we sought to establish a link between polycystin-1 (the *PKD1* gene product) and ATP-stimulated Cl^- secretion in renal tubule cells. To do this, we performed a whole cell patch-clamp analysis of the effects of expression of the isolated cytoplasmic COOH-terminus of polycystin-1 in stably transfected mouse cortical collecting duct cells. The truncated polycystin-1 fusion protein prolonged the duration of ATP-stimulated Cl^- conductance and intracellular Ca^{2+} responses. Both effects were dependent on extracellular Ca^{2+}. It was determined that expression of the truncated polycystin-1 fusion protein introduced, or activated, an ATP-induced Ca^{2+} entry pathway that was undetectable in transfection control cell lines. Our findings are concordant with increasing evidence for a role of polycystin-1 in cell Ca^{2+} homeostasis and indicate that dysregulated Ca^{2+} entry might promote Cl^- secretion and cyst expansion in ADPKD.

autosomal dominant polycystic kidney disease; purinergic P_2 receptors; chloride channels; kidney collecting tubules; patch-clamp techniques

IN THE MAJORITY OF CASES, autosomal dominant polycystic kidney disease (ADPKD) arises as a consequence of loss-of-function mutations in the polycystic kidney disease (*PKD1*) gene encoding polycystin-1 (11, 20). The cardinal feature of ADPKD is the gross disruption of normal renal parenchyma by multitudes of cysts. There is a close correlation between cyst expansion and loss of renal function (13), probably because cysts replace normal renal parenchyma and distort the renal vasculature as they grow.

ATP-stimulated Cl^- secretion may play a role in the accumulation of fluid required for cyst expansion. Stimulation of $P2Y_{2/4}$ purinergic receptors by extracellular ATP is a potent stimulus for Cl^- secretion in many epithelial systems, including renal tubule cell epithelia (4, 6, 9), and is mediated by phospholipase C, increased intracellular Ca^{2+} ion concentration ($[Ca^{2+}]_i$; see Ref. 39), and activation of Ca^{2+}-responsive Cl^- channels (possibly the Cl^-, Ca^{2+} channel; see Refs. 6 and 14). All the components for purinergic signal transduction have been identified within the ADPKD cyst, including: *1*) expression of $P2Y_2$ and other purinergic receptors in cyst epithelial cells, *2*) ATP release from cyst epithelial cells, and *3*) accumulation of ATP in the cyst lumen at micromolar levels (32). Cyst epithelial cells are responsive to extracellular ATP, which activates transepithelial Cl^- secretion through an increased $[Ca^{2+}]_i$ (32).

In a previous study, it was shown that expression of the cytoplasmic COOH-terminal 193 amino acids of polycystin-1 (the sIgPKD193 fusion protein) resulted in upregulation of ATP-stimulated transepithelial Cl^- secretion (19). In the present study, we show that the effect of the fusion protein on transepithelial Cl^- secretion is mediated by an increase in the amplitude and duration of ATP-stimulated Cl^- conductance and that the prolongation of Cl^- conductance is because of an effect of the sIgPKD193 fusion protein to upregulate agonist-stimulated Ca^{2+} entry. Our observations are the first to demonstrate that polycystin-1 pathways modulate ATP-stimulated Cl^- conductance through effects on Ca^{2+} entry and provide a plausible link between the genetic lesion and the relentless cyst expansion responsible for loss of renal function in ADKPD.

MATERIALS AND METHODS

Generation of stable cell lines. The M1 mouse cortical collecting duct cell line (33) was selected as the parental

Address for reprint requests and other correspondence: M. Sutters, Division of Renal Medicine, B2N, Johns Hopkins Bayview Medical Center, 4940 Eastern Ave., Baltimore, MD 21224 (E-mail: msutters@jhmi.edu).

The costs of publication of this article were defrayed in part by the payment of page charges. The article must therefore be hereby marked "*advertisement*" in accordance with 18 U.S.C. Section 1734 solely to indicate this fact.

source for stable transfections. We have already established that M1 cells express endogenous polycystin-1 mRNA (36). The sIgPKD193 construct (36) was created by fusion of a membrane expression cassette with the COOH-terminal cytoplasmic domain of murine polycystin-1 (provided by Drs. G. Waltz and G. Germino) and ligated into the glucocorticoid-responsive expression vector pLKNeo (18). Control lines were generated by stable transfections with the isolated membrane expression cassette (sIg) or vector alone.

For the purpose of this investigation, we used three dexamethasone (Dex)-inducible sIgPKD193-expressing cell lines referred to as clones 2, 18, and 20. Three control lines were created, known as sIg (expressing the membrane expression cassette alone) and p8 and p9 (both derived from vector-alone transfections). These cell lines have been described previously (19, 36). Expression of the sIgPKD193 fusion protein was evident by Western blot analysis in these cell lines, whereas endogenous full-length polycystin-1 expression was only detectable by prolonged exposure of Northern blot or by RT-PCR. This indicated that the sIgPKD193 fusion protein was probably present in excess over endogenous full-length polycystin-1.

Cell culture. Stably transfected M1 cells were used from passages 2–20 and were handled as already described (36). In brief, cells were grown on Matrigel-coated glass coverslips and maintained in a 5% CO_2 atmosphere at 37°C in DMEM-F-12 media (GIBCO) supplemented with 5% FCS (GIBCO). Where stated in the text, 1 μM Dex was added to the medium to induce fusion protein expression. Cells were seeded at 25,000 cells in 0.5-ml wells; the medium was changed to an FCS-devoid medium after 24 h of growth. Cells were used for electrophysiological and Ca^{2+}-measurement studies between 2 and 4 days after seeding. In preparation for each experiment, a complete panel of all six lines was seeded in each plate, thereby excluding systematic bias in the growth intervals. Ca^{2+}-imaging and patch-clamping studies were performed on identical-appearing single cells within clusters of ~25 cells. The cell morphology and degree of confluency were therefore no different between cell lines in patch-clamp or Ca^{2+}-imaging experiments. The cell capacitance measurements showed no difference between patched cells in the electrophysiological studies, indicating that there was no consistent variation in cell size between cell lines. We did not attempt to measure cilia length in these preparations but have noted the presence of apical cilia of similar appearance in all cell lines in separate studies of monolayers grown under identical circumstances.

General experimental design. Cells grown on glass coverslips were superfused (5 or 2 ml/min for patch-clamp or fluorescence studies, respectively) by a continuous-flow system that allowed quick addition and washout. Agonists were added for 10 s in patch-clamp studies and for 20 s in single-cell fluorescence studies and then washed for a period of 10 min in experiments requiring repeated stimulation. The majority of experiments were performed at room temperature, but one experiment was performed at 34–36°C using a heated stage to confirm that the effect of fusion protein expression on the ATP-stimulated Ca^{2+} response was evident at physiological temperature.

Patch-clamp technique. The perforated-patch whole cell configuration of the patch-clamp technique was used. To establish the perforated patch, 10 μM β-escin was added to the pipette solution (12). An Axopatch 200B patch-clamp amplifier (Axon Instruments) and computer complete with pCLAMP 8.0 software (Axon Instruments) were used to acquire and analyze whole cell currents (I) or membrane voltage. Cells were viewed through the ×40 objective of a Nikon inverted microscope. Patch pipettes were pulled from Kwik-Fil glass capillaries (World Precision Instruments) and had a resistance ranging between 3.5 and 4.0 MΩ. The reference electrode was an Ag/AgCl pellet. Current signals were filtered at 5 kHz and displayed on an oscilloscope (20 MHz digital storage, type 1425; Gould). Agonist-activated membrane currents at a holding potential (V_h) of −60 mV were recorded at room temperature (21–23°C).

mRNA extraction. mRNA extraction and RT-PCR methods are as described previously (3). Briefly, M1 cell monolayers were resuspended in 1 ml TRIzol reagent (GIBCO-BRL) and passed through a pipette several times to ensure a homogeneous suspension. RNA was extracted using TRIzol/chloroform extraction and isopropyl alcohol precipitation according to the manufacturer's protocol. The final pellet was air-dried and resuspended in RNase-free distilled water. RNA concentration and purity were determined by spectrophotometry.

RT-PCR. Specific primers were selected from the sequence of the mouse $P2Y_2$, $P2Y_4$, and $P2Y_6$ receptor cDNA by using Oligo Primer analysis software (Medprobe, Oslo, Norway). RT-PCR methods were as described previously (3). Briefly, 1 μg total RNA was reverse transcribed for 50 min at 42°C with 0.5 μl oligo$(dT)_{12-18}$ using a first-strand cDNA synthesis kit for RT-PCR (Superscript II RNase H^- RT; GIBCO-BRL). Negative controls were carried out in the absence of RT. The resulting cDNA template or negative control (10%) was used for PCR amplification with PCR Core System I (Promega, Southampton, UK) following the manufacturer's instructions. For all experiments, denaturation at 95°C for 3 min was followed by 30 cycles of 95°C for 30 s, annealing for 1 min and 72°C for 1 min, and then a final extension step of 72°C for 5 min. PCR products were resolved on a 2% (wt/vol) agarose gel containing 10 μg/ml ethidium bromide and visualized under ultraviolet illumination. Images were captured using a Fluor-S Multi-Imager (Bio-Rad). The primer sequences used were as listed as follows: $P2Y_2$, CTTCAAGTACGTGCTGTTGC (forward) and AGGTGTCATGGCAAGTGATC (reverse); $P2Y_4$, GCTATTCACATCACTAGGTC (forward) and GCAGTAGAGGTTCCAGTAGA (reverse); $P2Y_6$, GGCTTGTTATTGTCGCA (forward) and GCCTCTGTAAGAGATCGT (reverse).

The annealing temperatures and product size for each reaction were as follows: $P2Y_2$, 58°C and 470 bp; $P2Y_4$, 58°C and 331 bp; $P2Y_6$, 56°C and 329 bp.

Measurement of $[Ca^{2+}]_i$. A spectrofluorometric method with fluo 3-AM (dissolved in DMSO with 20% pluronic acid) as the Ca^{2+} indicator was used for measurement of $[Ca^{2+}]_i$ in single cells. Cells were loaded with 10 μM fluo 3-AM in DMEM-F-12 medium for 30 min at room temperature (21–23°C). Cells were then washed thoroughly with medium to remove extracellular fluo 3-AM and rested for 30–45 min to allow for complete deesterification of cytosolic dye. Fluo 3-AM was excited at 488 nm with a xenon light source, and fluorescence was measured at 535 nm, recorded, and stored in a computer for data processing and analysis using pCLAMP 8.0 software. Photo bleaching and light-induced damage to cells were minimized by taking short measurements (of 120-ms duration) one time per second over a 200-s period. Studies were performed at room and physiological temperatures. On analysis, fluorescence data for each experiment were normalized to the individual basal fluorescence value to bring all the response curves to the same pretreatment starting point. Equivalent loading of cells was confirmed by incubation with the Ca^{2+} ionophore A-23187 (10 μM) and measurement of fluorescent signal in response to perfusion with a solution containing 10 mM Ca^{2+} (maximal) and subsequent quenching in 1 M manganese chloride (background). There

were no consistent differences between cell lines with respect to the basal fluorescence values or efficiency of loading with fluo-3 AM. Fluorescent signal intensity was attenuated when cells were studied at 34–36°C, where a down-sloping baseline indicated progressive loss of cytoplasmic dye as the probable explanation. Because of this, single-cell studies were not possible at physiological temperature, and, consequently, groups of ~25 cells were imaged in the studies at the warmer temperature to increase the signal-to-noise ratio.

Measurement of Ca^{2+} influx. To measure Ca^{2+} influx after a Ca^{2+} release stimulus, cells were loaded with fluo 3-AM as described above and stimulated with 10 μM ATP for 30 s in a zero Ca^{2+} buffer to prevent refilling of the endoplasmic reticulum (ER) from capacitative Ca^{2+} entry. Three minutes following exposure to ATP, cells were switched to a buffer containing 2 mM Ca^{2+} (Ca^{2+} add-back). In each experiment, a field of ~50 cells was imaged continuously. The absolute increase in fluorescent signal on Ca^{2+} add-back was taken as an indicator of the degree of activation of Ca^{2+} entry pathways. Because exposure to zero Ca^{2+} buffer might itself promote Ca^{2+} entry (7), baseline studies of the effect of transition from zero to normal external Ca^{2+} were performed. Ca^{2+} add-back responses are expressed as the peak fluorescent signal minus the value immediately preceding Ca^{2+} add-back.

Solutions. The standard bath solution was (in mM) 140 NaCl, 5 KCl, 1.8 $MgCl_2$, 1.8 $CaCl_2$, and 10 HEPES (adjusted to pH 7.45 with NaOH). For the evaluation of fluo-3 AM loading efficiency, the Ca^{2+} concentration of this buffer was increased to 10 mM. For the zero Ca^{2+} buffer, Ca^{2+} was replaced with 0.1 mM EGTA. In patch-clamp experiments, microelectrode pipettes were filled with (in mM) 140 KCl, 1.8 $MgCl_2$, and 10 HEPES (adjusted to pH 7.4 with KOH and filter sterilized). β-Escin (10 μM) was added to the final pipette solution. All chemicals and reagents were purchased from Sigma, except for fluo 3-AM, which was obtained from Molecular Probes. Antagonists were preincubated for 10 min before the addition of ATP (~EC_{70} concentration, 3 μM ATP). The reversibility of receptor blockade was tested after a 10-min antagonist-washout period.

Data analysis. For concentration-response curves, data were normalized to the maximum current (I_{max}) evoked by ATP (10 μM). The agonist concentration that evoked 50% of the maximum response (EC_{50}) was taken from Hill plots of the transform, $\log(I/I_{max} - I)$. Concentration-response curves were fitted by nonlinear regression analysis using commercial software (Prism version 2.0; Graph-Pad). Decay times were calculated as the time for the ATP-induced current or cell Ca^{2+} response to fall from 80 to 20% of the peak value. Multiple comparisons between the six cell lines were made by one-way ANOVA, with significance accepted at $P < 0.05$ by unpaired two-tailed *t*-test with the Dunnett multiplicity adjustment, using "Instat II" software. Comparison between the two groups of cell lines (control vs. sIgPKD193) was made by unpaired *t*-test. Data are given as mean values ± SE for *n* experiments.

RESULTS

Whole cell patch-clamp experiments. ATP elicited a whole cell, inward Ca^{2+}-activated Cl^- current in voltage-clamped ($V_h = -60$ mV) M1 mouse cortical collecting duct-derived cell lines. Six cell lines were studied (3 sIgPKD193-expressing cell lines, named clone 2, 18, and 20; and 3 control cell lines named sIg, p8, and p9). After treatment with 1 μM Dex, the maximal ATP-induced currents were greater in the sIgPKD193 fusion protein-expressing clones 2, 18, and 20 ($P < 0.005$). This effect is shown in representative traces for sIg (control cell line) and clone 18 (sIgPKD193-expressing cell line) in Fig. 1*A* and summarized in Fig. 1*B*. In the absence of Dex, peak currents were no different between cell lines. As can be seen in representative whole cell current responses to ATP (Fig. 1*A*) and in summary data (Fig. 1*C*), expression of the sIgPKD193 fusion protein significantly increased the decay time of ATP-evoked whole cell currents ($P < 0.0001$). In the absence of Dex treatment, decay rates were similar in all cell lines. There were no differences between cell lines in activation rates irrespective of treatment with Dex (data not shown).

The ATP concentration-response relationships for clones sIg and 18 were identical in the presence and absence of Dex (Fig. 2*A*), indicating that there was no effect of Dex or fusion protein expression on receptor sensitivity to agonist activation. A range of nucleotide agonists was tested for activity in the control cell line (sIg, plus Dex) and the sIgPKD193 clone (18, plus Dex) to test whether expression of the sIgPKD193 fusion protein resulted in a change in receptor subtype expression (Fig. 2*B*). The agonists used were ATP, UTP, 2-methylthio-ATP (2-meSATP), and 2′3′-*O*-(4-benzoylbenzoyl)-ATP (BzATP). The potency order for both sIg and 18 (by comparison of EC_{50} values) was ATP = UTP > 2-meSATP > BzATP. In both cases, 2-meSATP and BzATP were partial agonists. The same results were found in the absence of Dex treatment (data not shown). This pharmacological profile was consistent with the presence of $P2Y_2$, $P2Y_4$, and/or $P2Y_6$ receptors (all responsive to uridine compounds). RT-PCR analysis performed on parental M1 cells confirmed expression of mRNA for each of these purinergic receptor subtypes (Fig. 2*C*).

The current response to ATP was characterized with respect to the reversal potential and antagonist profile, as shown in Fig. 3, *A* and *B*. Current-voltage analysis was performed, in conditions symmetric with respect to Cl^-, Mg^{2+}, and HEPES, on ATP-evoked currents (10 μM, EC_{100} value) in Dex-treated cell lines sIg and 18. These studies yielded near-zero reversal potentials. Treatment with the P2 antagonist pyridoxalphosphate-6-azophenyl-2′,4′-disulfonic acid (PPADS; 100 μM) blocked ATP-evoked currents equally in sIg and 18, as did the Cl^--channel blocker DIDS (100 μM). The current-voltage analysis and response to DIDS indicated that the current was carried by Cl^-.

As demonstrated by others, the effect of ATP on Cl^- conductance is mediated by increased cell Ca^{2+} (6, 9, 31). ATP-stimulated cell Ca^{2+} responses are biphasic, with an initial peak resulting from Ca^{2+} release from the ER, followed by a more prolonged phase resulting from Ca^{2+} entry from outside the cell (5). The latter component, described as "store-operated" Ca^{2+} entry, is thought to be triggered by ER Ca^{2+} store depletion and serves as the means of replenishing these Ca^{2+} stores (30). The prolongation of the decay phase of the ATP-stimulated current induced by expression of the sIgPKD193 fusion protein therefore suggested that the

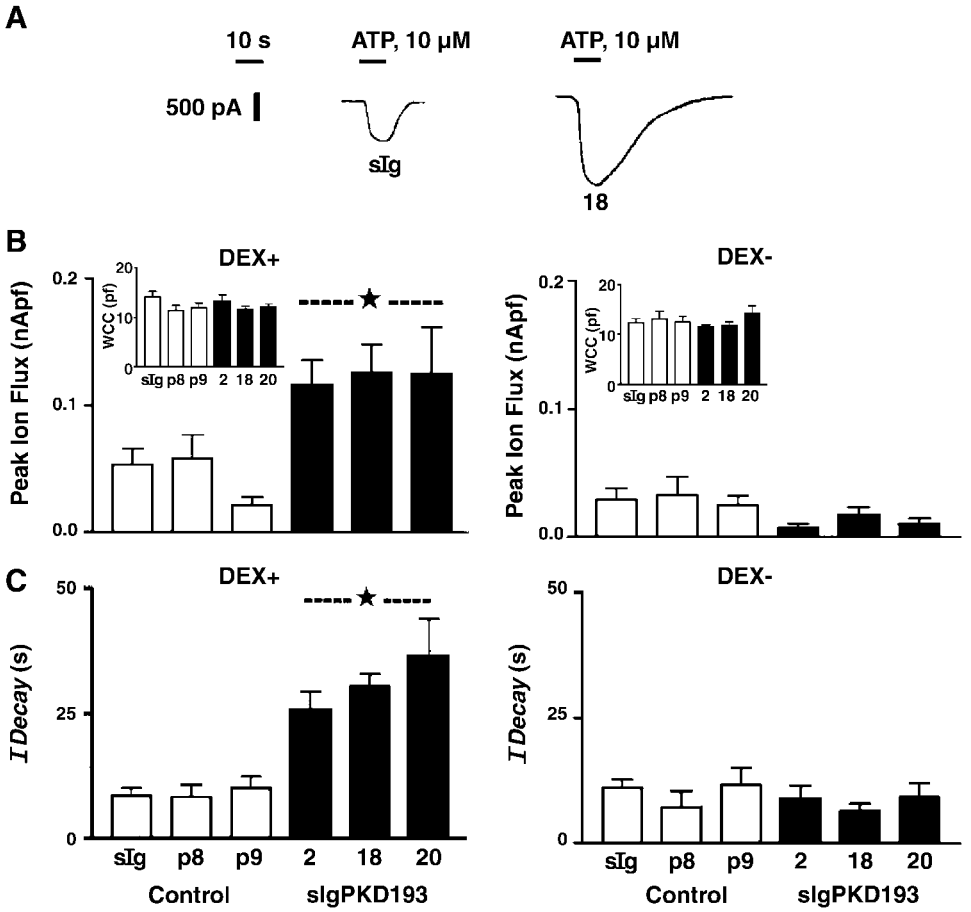

Fig. 1. Expression of the sIgPKD193 fusion protein resulted in an increase in the peak and duration of the ATP-stimulated whole cell Cl^- current response of a cortical collecting duct cell line. *A*: representative whole cell patch-clamp tracing in Dex-treated cells shows that the amplitude and duration of the whole cell ion flux response to ATP were increased in a cell expressing the sIgPKD193 fusion protein (clone 18) compared with a transfection control cell (sIg). *B*: in a series of such experiments, peak ion flux in response to ATP was significantly increased ($P < 0.005$) by expression of the sIgPKD193 fusion protein in 3 stably transfected cell lines. In the absence of dexamethasone (Dex), peak ion flux was no different between cell lines. *Inset* shows whole cell capacitance (WCC), which was similar in all cell lines. *C*: prolongation of the ATP response in cells expressing the sIgPKD193 fusion protein can be clearly seen as an increase in the time taken for decay from 80 to 20% of the ATP-induced peak current ($P < 0.0001$). In the absence of Dex, there was no difference in decay time between cell lines. The number of observations for each experiment is as follows (listed as sIg, p8, p9, 2, 18, and 20): Dex+: 15, 10, 8, 10, 15, and 5; Dex−, 8, 6, 6, 6, 6, and 6. *I*, current. ⋆Significant difference from control.

truncated polycystin-1 fusion protein might have upregulated store-operated Ca^{2+} entry. Consistent with this possibility, removal of bath Ca^{2+} by EGTA (0.1 mM) had no effect on control clone sIg but shortened the decay phase of the ATP response to a control configuration in sIgPKD193-expressing clone 18 (Fig. 3*C*). This effect was partially reversed after a 10-min washout of EGTA, revealing a biphasic decay of Cl^- current in clone 18. Measurements of $[Ca^{2+}]_i$ were therefore made to explore the possibility that altered

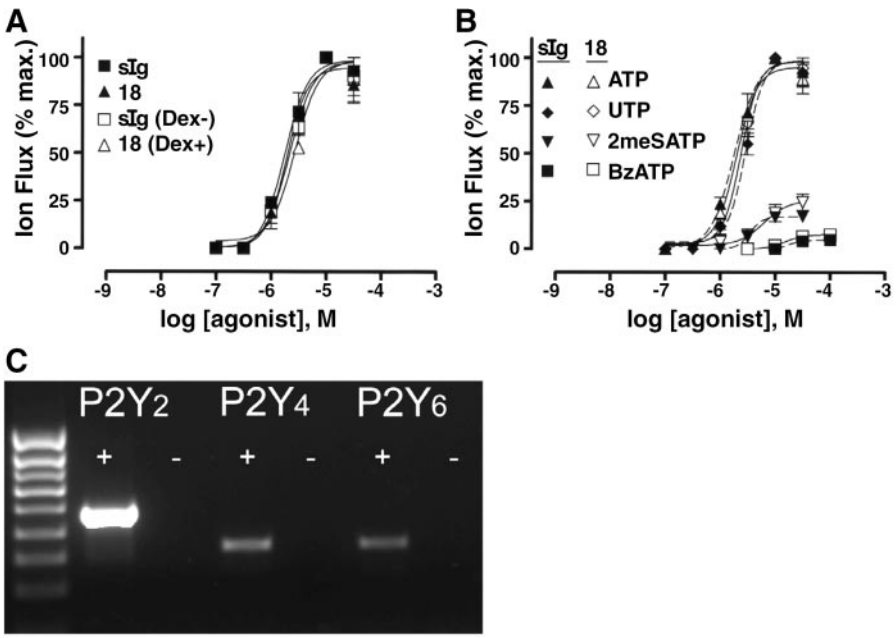

Fig. 2. Expression of the sIgPKD193 fusion protein had no effect on the pharmacodynamics of the purinergic response. *A*: whole cell patch-clamp ATP concentration-response curves were the same, irrespective of Dex treatment, in cell lines sIg (control, $n = 4$) and 18 (which expresses the sIgPKD193 fusion protein in response to Dex, $n = 6$). *B*: whole cell patch-clamp agonist concentration-response curves for Dex-treated cell lines sIg and 18 ($n = 4$, both cell lines) showed that both cell lines responded in similar fashion to a range of purinergic agonists. 2-meSATP, 2-methylthio-ATP; BzATP, 2′3′-*O*-(4-benzoylbenzoyl)-ATP. *C*: RT-PCR analysis of M1 parental cells showed expression of $P2Y_2$, $P2Y_4$, and $P2Y_6$ receptors. Product was detected in the RT positive (+) but not in the RT negative (−) lanes.

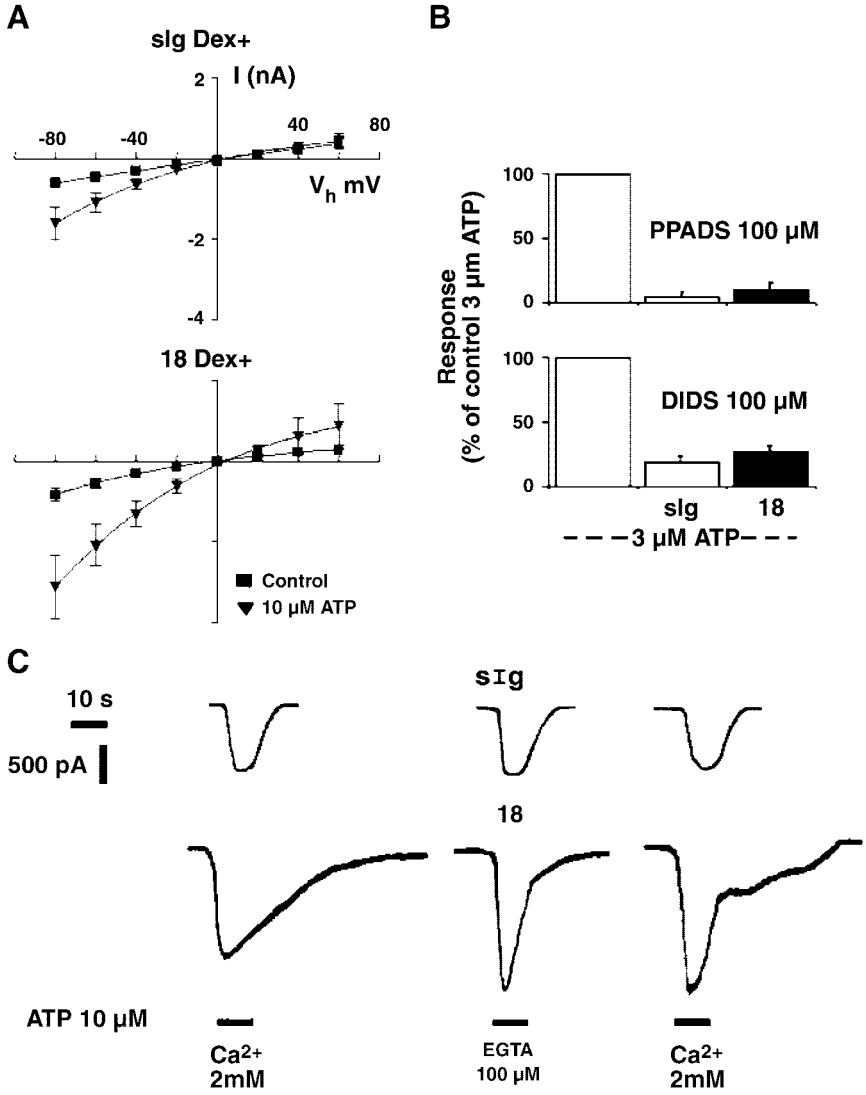

Fig. 3. Characterization of the ATP-induced current. *A*: current (I)-voltage (V_h) relationship of the ATP response in Dex-treated sIg and 18 (n = 6 for both cell lines) passed through 0, which, in symmetric Cl^- conditions, indicated that ATP was activating a membrane Cl^- conductance. *B*: ATP response was blocked by pyridoxalphosphate-6-azophenyl-2′,4′-disulfonic acid (PPADS) and by DIDS, consistent with the involvement of $P2Y_{2/4}$ purinergic receptors and Ca^{2+}-activated Cl^- channels (n = 4 for each experiment). *C*: representative (of 4 separate experiments) whole cell patch-clamp recordings of 3 consecutive responses to ATP in Dex-treated cells. The ATP response of the control cell line (sIg) was unaffected by withdrawal of bath Ca^{2+} (EGTA). By contrast, withdrawal of bath Ca^{2+} converted the prolonged response of clone 18 to a shortened response typical of the control cell lines (compare with sIg tracing). In the third tracing of 18, return of bath Ca^{2+} for 10 min partially restored the prolonged response, resulting in a pattern indicating a fusion between the external Ca^{2+}-independent and -dependent phases.

cell Ca^{2+} responses could have explained the effect of the sIgPKD193 fusion protein on ATP-stimulated Cl^- conductance.

Fluorescence Ca^{2+} measurements. Changes in $[Ca^{2+}]_i$ were measured in single cells after treatment with 1–100 μM ATP in the presence and absence of Dex. ATP (10 μM) yielded the maximal fluorescence increase across all cell lines. Mean single-cell basal and maximum ATP-stimulated fluorescence values were the same for the two groups of cell lines (basal: controls = sIgPKD193 = 0.0012, maximal ATP stimulated: controls = sIgPKD193 = 0.002, all expressed as nonnormalized arbitrary units). Activation times were calculated from 20 to 80% of the rise time of the curve as follows: 27.4 ± 5.5 s (n = 5), 21.9 ± 2.5 s (n = 4), and 25.9 ± 2.0 s (n = 5), for sIg, p8, and p9 and 23.7 ± 1.5 s (n = 6), 22.6 ± 1.2 s (n = 11), and 26.7 ± 1.7 s (n = 7) for clones 2, 18, and 20 (+Dex), respectively. Activation times were not significantly different between cells expressing the sIgPKD193 fusion protein and control cells. Dex-induced expression of the sIgPKD193 fusion protein caused an increase in the 80–20% decay time of the $[Ca^{2+}]_i$ response in sIgPKD193 cell lines (as shown for clone 18 in Fig. 4*A*) that resembled the effect seen with Cl^- current in the patch-clamp experiments. Dex had no such effect in control cells (as shown for clone sIg in Fig. 4*A*). There were no differences in decay time between cell lines in the absence of Dex treatment. The effect of fusion protein expression on decay time was consistently seen in comparisons between all sIgPKD193 and control cell lines, as summarized in Fig. 4*B*. Single cell $[Ca^{2+}]_i$ responses to ATP had a longer duration than the single cell current responses. This could be explained in a number of ways, since Cl^- channel inactivation is regulated by non-Ca^{2+}-dependent mechanisms. For example, Ca^{2+}-activated Cl^- channels exhibit voltage-dependent Ca^{2+} sensitivity (24) and are inactivated after ATP stimulation by parallel induction of tetrakiphosphate synthesis (8). Removal of bath Ca^{2+} (0 Ca^{2+}, 0.1 mM EGTA, Fig. 5) had no detectable effect on the $[Ca^{2+}]_i$ response of control clone sIg but decreased the $[Ca^{2+}]_i$ decay time in clone 18, transforming it to a control-type response. The effect of EGTA on the $[Ca^{2+}]_i$ response to ATP was

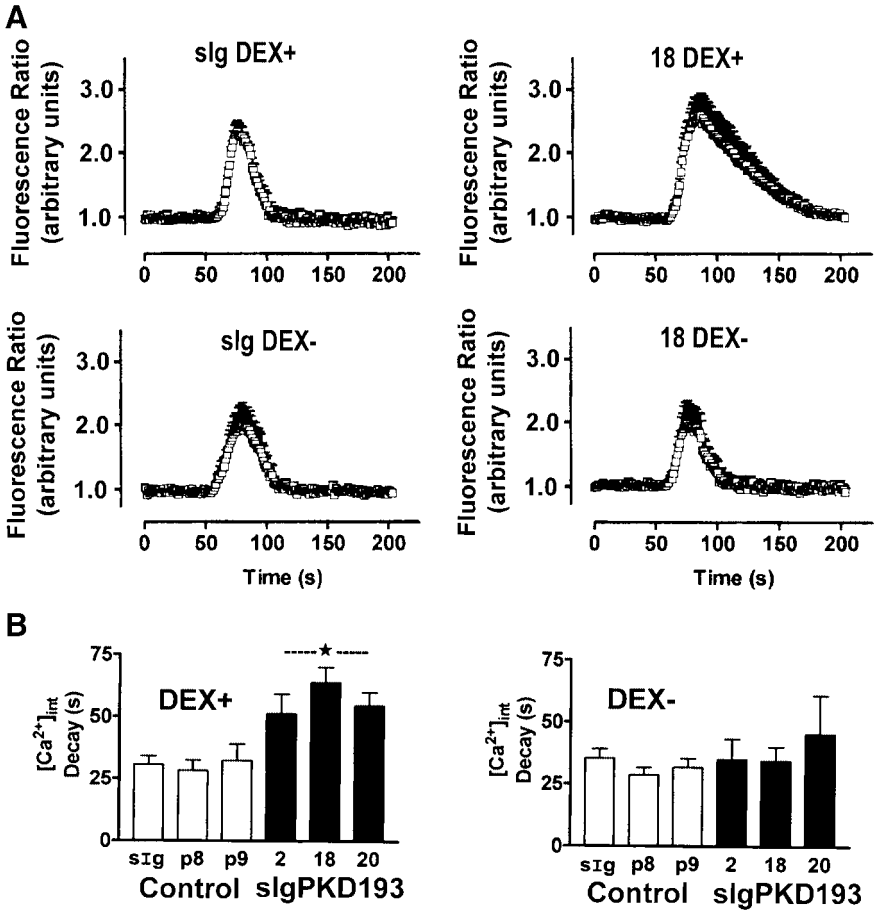

Fig. 4. Dex-induced expression of the sIgPKD193 fusion protein resulted in prolongation of the single-cell Ca^{2+} response to ATP. *A*: fluorescence intracellular Ca^{2+} responses (mean ± SE) to ATP were measured in single cells with the Ca^{2+} indicator fluo 3-AM in a control (sIg: Dex+ $n = 5$, Dex− $n = 4$) and a sIgPKD193 cell (18: Dex+ $n = 7$, Dex− $n = 3$). Dex-induced expression of the sIgPKD193 fusion protein caused a prolongation of the decay time of the ATP response. In the absence of Dex, the ATP responses of the cell lines were indistinguishable. *B*: results for a series of studies of the single-cell Ca^{2+} response to ATP in all cell lines. Dex-induced expression of the sIgPKD193 fusion protein resulted in a significant prolongation of the decay time in cell lines 2, 18, and 20 ($P < 0.001$). $[Ca^{2+}]_i$, intracellular Ca^{2+} concentration. The no. of observations for each experiment is as follows (in the order sIg, p8, p9, 2, 18, and 20): Dex+, 5, 3, 5, 6, 7, and 7; Dex−, 4, 3, 3, 6, 3, and 4.

reversible within 30 min (data not shown). Hence, the prolongation of decay of ATP-induced current and $[Ca^{2+}]_i$ was dependent on fusion protein expression and the presence of Ca^{2+} in the extracellular medium. The absence of an effect of Ca^{2+} withdrawal on the ATP-induced $[Ca^{2+}]_i$ response of the control cell lines suggested that the contribution made by store-operated Ca^{2+} entry to the $[Ca^{2+}]_i$ curve was small and not resolvable in these cells by the fluorescent Ca^{2+} protocols employed in these studies. ATP-evoked (10 μM) changes in $[Ca^{2+}]_i$ were also modulated by the addition of PPADS (100 μM), where the fluorescence ratio increase was reversibly inhibited by 53.4 ± 9.6% ($n = 3$) in sIg (+Dex) and 61.1 ± 12.4% ($n = 3$) in clone 18 (+Dex); these values were not significantly different in the absence of Dex. DIDS (100 μM) had no effect on $[Ca^{2+}]_i$ levels in any of the clones, irrespective of Dex treatment ($n = 3$ for each experimental group, data not shown).

To dissociate Ca^{2+} release from Ca^{2+} entry, $[Ca^{2+}]_i$ was measured on return of Ca^{2+} to the bath 3 min after stimulation with ATP in zero Ca^{2+} buffer. The increase in fluorescence signal indicated Ca^{2+} influx, which was activated by transition from 0 to 2 mM Ca^{2+} alone in baseline (non-ATP-treated) experiments (Fig. 6*A*). Interestingly, prior stimulation of Dex-treated cells with ATP did not increase the Ca^{2+} influx response above basal in control cells but evoked a significant supra-basal increase in Ca^{2+} influx in cells expressing the sIgPKD193 fusion protein (Fig. 6, *B* and *D*, $P = 0.0052$). Control cell line responses were the same in Dex plus vs. Dex minus experiments, whereas the effect of ATP on the Ca^{2+} entry response in the sIgPKD193 cell lines was reduced (although not completely to control cell line levels) in the absence of Dex (Fig. 6, *B*, *C*, and *D*, $P = 0.048$). Peak ATP responses in the absence of Ca^{2+} were not significantly different in these experiments.

DISCUSSION

In the whole cell patch-clamp experiments presented in this study, we have shown that expression of the cytoplasmic COOH-terminal 193 amino acids of murine polycystin-1 upregulated an ATP-induced Cl^- current. The sIgPKD193 fusion construct was introduced in these cell lines under the influence of a Dex-responsive element; induction of sIgPKD193 fusion protein expression by treatment with Dex resulted in an increase in peak ATP-induced current and significantly prolonged the ATP response in the sIgPKD193 cell lines but had no effect on the ATP-induced current in control lines. In the absence of Dex, there was no difference in the ATP-induced currents between control and sIgPKD193 cell lines. Analysis of current-voltage relationships demonstrated that the modu-

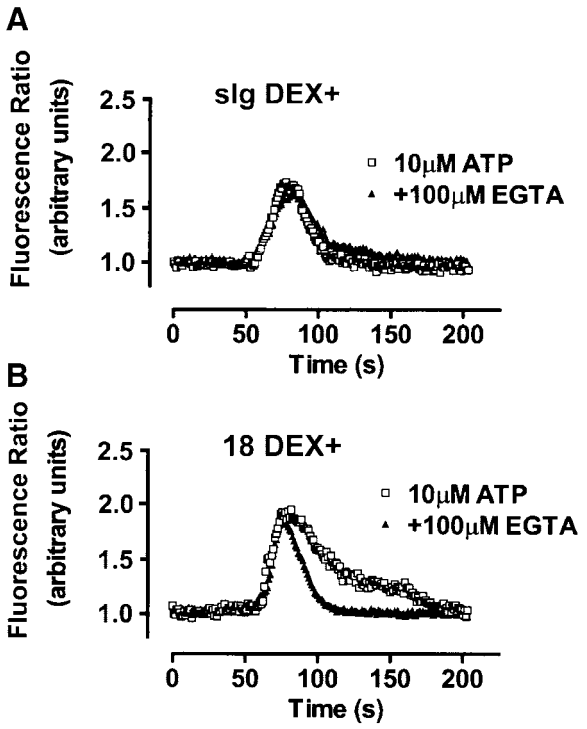

Fig. 5. Prolongation of ATP-induced cell Ca^{2+} response associated with expression of the sIgPKD193 fusion protein was dependent on bath Ca^{2+}. *A*: in the representative individual cell tracing of a Dex-treated control (sIg) cell Ca^{2+} response to ATP, the switch to 0 Ca^{2+} (EGTA) had no effect on the ATP-induced cell Ca^{2+} response. The representative tracing in *B* shows the characteristic prolongation of inactivation time in the ATP-induced Ca^{2+} response in the presence of Ca^{2+} in a cell expressing the sIgPKD193 fusion protein (18), and the transformation to a control pattern in this cell in 0 bath Ca^{2+} (EGTA). Results are representative of 3 experiments for each cell line. Activation times varied from cell line to cell line, independently of expression of the sIgPKD193 fusion protein (see RESULTS for these values).

lated current was mediated by Cl^-. The current was completely and irreversibly inhibited by DIDS, consistent with involvement of a Ca^{2+}-activated Cl^- channel. UTP and ATP demonstrated similar concentration-response curves, and these responses were reversibly inhibited by PPADS, indicating that the ATP response was most probably the result of activation of $P2Y_2$ and/or $P2Y_4$ purinergic receptors. The involvement of these two P2Y subtypes is inferred by the following observations. The murine isoforms of both are activated by ATP and UTP (26, 34). 2-meSATP and BzATP are partial agonists at the murine $P2Y_2$ receptor (10), but this subtype is relatively insensitive to PPADS, whereas murine $P2Y_4$ is particularly sensitive to this P2 receptor antagonist (34). None of the other known P2Y receptor subtypes (23) fits the pharmacological profile of the endogenous P2Y receptor(s) in mouse M1 cells. In keeping with this interpretation, RT-PCR analysis of M1 parental cells showed expression of both $P2Y_2$ and $P2Y_4$ mRNA.

Expression of the sIgPKD193 fusion protein did not alter the agonist pharmacological profile of the response, indicating that the effect on ATP-stimulated Cl^- conductance did not appear to be mediated through an alteration in the expression pattern of purinergic receptor subtypes. Expression of the fusion protein did not appear to have wider nonspecific effects on these cells, since the resting membrane potential, basal currents, and whole cell capacitance were similar in the two groups of cell lines.

Expression of the sIgPKD193 fusion protein increased the peak of the ATP response but also significantly slowed the recovery to baseline current after washout. As other investigators have shown (5), the effect of extracellular ATP on cell Ca^{2+} is biphasic, with an early peak attributable to Ca^{2+} release from the ER and a more sustained phase that is probably triggered by a subsequent period of Ca^{2+} entry from the extracellular solution, termed the store-operated phase (30). ATP-induced changes in cell Ca^{2+} are responsible for the effect of ATP on Cl^- channel activation (6, 9, 31). We show in the present paper that the sIgPKD193 fusion protein-induced prolongation of ATP-induced Cl^- current was probably the consequence of upregulation of store-operated Ca^{2+} entry. The evidence for this was fourfold. *1*) Removal of bath Ca^{2+} before stimulation with ATP resulted in acceleration of the decay in current, transforming the ATP response of the sIgPKD193-expressing cell lines to a control pattern. This manipulation did not affect the ATP response of the control cell lines. *2*) The $[Ca^{2+}]_i$ response to ATP was prolonged in the sIgPKD193-expressing cell lines. *3*) As was seen with the ATP-stimulated Cl^- current, withdrawal of bath Ca^{2+} returned the $[Ca^{2+}]_i$ response to a control pattern. *4*) The Ca^{2+} add-back studies demonstrated that expression of the sIgPKD193 fusion protein introduced, or activated, an ATP-dependent Ca^{2+} entry pathway that was not detectable in the control cell lines. This Ca^{2+} entry pathway persisted to a lesser extent in the sIgPKD193 cells in the absence of Dex but was significantly increased by Dex treatment only in the sIgPKD193 cell lines. The persistence of the effect in the absence of Dex could be explained by background leak of fusion protein expression in noninduced cells (19) and was of insufficient magnitude to appreciably affect the current or cell Ca^{2+} responses recorded in the absence of Dex in the single cell experiments.

Unexpectedly, although the peak amplitude of the whole cell current response was increased in cells expressing the sIgPKD193 fusion protein, we could detect no corresponding difference in the peak amplitude of the single-cell Ca^{2+} responses. Thus there was no evidence, in our experimental model, for an effect of the sIgPKD193 fusion protein to increase ER Ca^{2+} release. If ER release was not affected by the sIgPKD193 fusion protein, then the fusion protein might have upregulated the ATP-induced peak current through increased cell responsiveness to the initial phase of Ca^{2+} release from the ER, but we have not addressed this issue in the current studies.

Aguiari et al. (1) also found that expression of the truncated COOH-terminus of polycystin-1 in human embryonic kidney (HEK-293) cells increased the cell

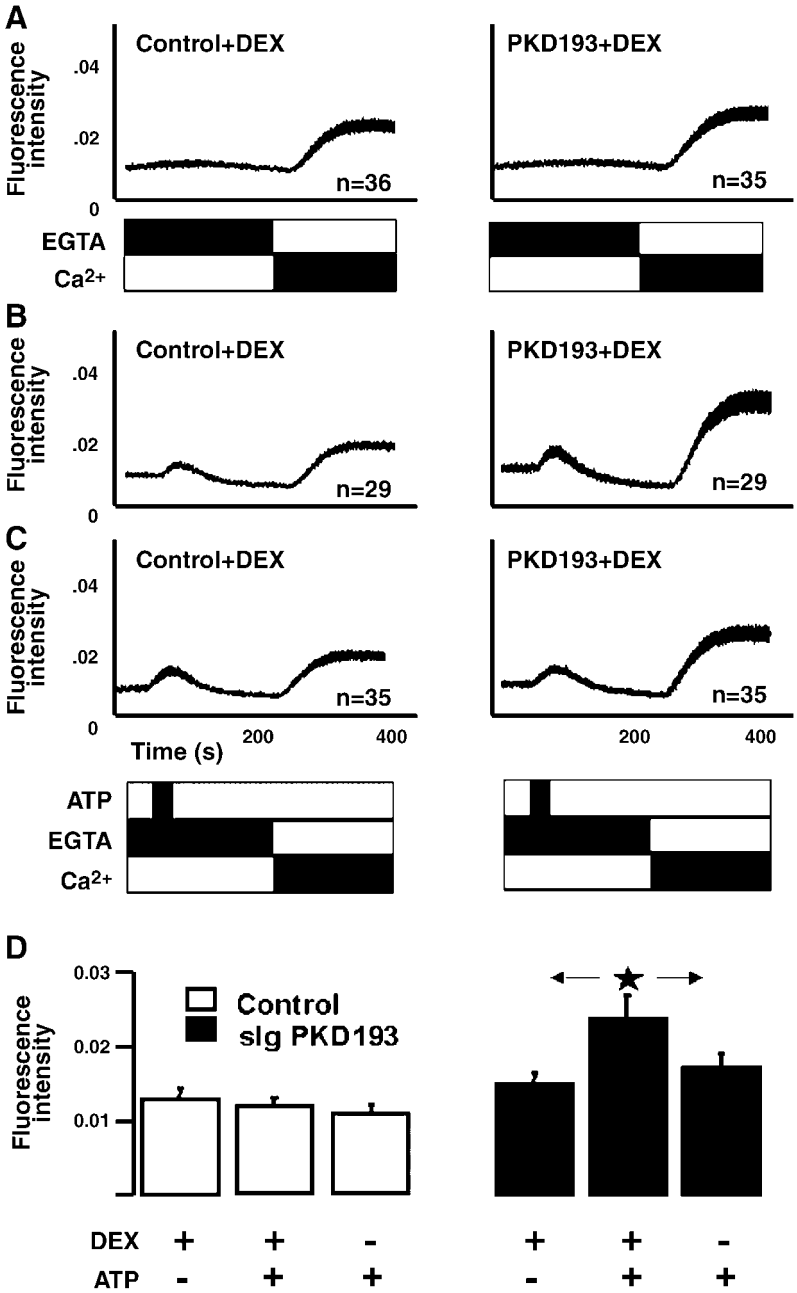

Fig. 6. Expression of the sIgPKD193 fusion protein evoked an ATP-stimulated Ca^{2+} entry pathway that was not detectable in control cell lines. Cell Ca^{2+} was measured in groups of cells loaded with the Ca^{2+}-sensitive dye fluo 3-AM. Data are presented as absolute fluorescence intensity. *A*: in the baseline (non-ATP-treated) experiment, Dex-treated cells were perfused for 3.5 min in a 0 Ca^{2+} buffer (EGTA) and then switched to a buffer containing 2 mM Ca^{2+}. Increased fluorescent signal indicated Ca^{2+} influx in response to the transition from 0 to 2 mM Ca^{2+} (Ca^{2+} add-back). *B*: treatment with ATP in the 0 Ca^{2+} buffer had no effect on the subsequent Ca^{2+} add-back response relative to the basal response in Dex-treated control cells but increased the Ca^{2+} add-back response above basal in cells expressing the sIgPKD193 fusion protein. *C*: withdrawal of Dex had no effect on the Ca^{2+} add-back response of the control cells but reduced that of the sIgPKD193 cells relative to their Dex-treated response. These results are summarized in *D*, where the response to the switch to 2 mM Ca^{2+} is depicted as the magnitude of increase in fluorescence from levels immediately before Ca^{2+} add-back. ATP had no effect on Ca^{2+} entry in control cells (relative to the basal response), irrespective of Dex treatment. By contrast, the response of the sIgPKD193 cell lines was increased after ATP in the Dex+ experiments (plus vs. minus ATP, $P = 0.0052$). In the ATP+ experiments, Dex increased the magnitude of the Ca^{2+} add-back response in sIgPKD193 cell lines (plus vs. minus Dex, $P = 0.048$) but had no effect on this response in control cell lines. The total no. of observations for each experiment are listed below the curves in *A*, *B*, and *C*. Equal numbers of each cell line (±1) were pooled in the control and PKD193 groups in each experiment. The curves plotted in *A*, *B*, and *C* depict the range ± SE for each point. ⋆Significant difference between *middle* vs. flanking bars.

Ca^{2+} response to ATP. However, in contrast to our findings, these authors concluded that the truncated fusion protein was increasing cell Ca^{2+} responses via an effect on ER Ca^{2+} release. This conclusion was based on parallel experiments in stably transfected HeLa cells treated with histamine, but the effect of the fusion protein on peak histamine-stimulated $[Ca^{2+}]_i$, whether in the presence or absence of bath Ca^{2+}, seemed marginal in the data presented by these authors. In fact, their figures showed that the truncated polycystin-1 fusion protein introduced a plateau to the ATP-induced Ca^{2+} response in HEK cells and suggested that the fusion protein increased store-operated Ca^{2+} entry induced by histamine in HeLa cells. We have directly demonstrated that the truncated polycystin-1 fusion protein augmented Ca^{2+} entry after treatment with ATP in a well-characterized collecting duct-derived cell line. Furthermore, we have established that this may represent a mechanism of disease, for the first time linking disturbance of polycystin pathways to the prolongation of an ATP-stimulated Cl^- current. Aguiari et al. found that expression of the truncated polycystin-1 fusion protein increased the peak amplitude of Ca^{2+} responses, whereas we found no such effect. Our single-cell studies were performed at room temperature, and those of Aguiari et al. were performed at 37°C; therefore, to exclude the possibility that the truncated polycystin-1 fusion protein might only increase the amplitude of Ca^{2+} responses at the warmer temperature, we repeated a series of ATP-

induced Ca^{2+} responses at physiological temperatures. As seen in the original experiments, the cell Ca^{2+} responses remained prolonged in cells expressing the PKD193 fusion protein studied at 34–36°C (the time taken for the decline from 80 to 20% of the peak response was 29 ± 1.8 s in control vs. 38 ± 3.2 s in PKD193-expressing cells, $P = 0.037$, $n = 11$ and $n = 16$ respectively), and peak Ca^{2+} responses were not increased in cells expressing the PKD193 fusion protein studied at the physiological temperature (fluorescence ratio: control 0.722 ± 0.109, PKD193-expressing cells 0.561 ± 0.117, $n = 11$ and 16, respectively). We have no definitive explanation for the differences in peak responses between the two studies, but it is possible that the truncated polycystin fusion protein exhibits cell type-specific effects. Alternatively, this difference might have arisen from compartmentalization, since the bioluminescent protein aequorin (the Ca^{2+} indicator used by Aguiari et al.) might not share the same cell distribution as the Ca^{2+} indicator dye fluo 3. In any case, the peak Ca^{2+} response is, at best, an indirect indicator of ER Ca^{2+} release and might be influenced by other Ca^{2+} fluxes arising from within or outside the cell.

In another recent study, Nauli et al. (27) described the cell Ca^{2+} response to thrombin in distal renal tubule cells derived from a transgenic mouse with a targeted deletion of exon 34 of the *PKD1* gene (25). Interestingly, loss of polycystin-1 function in these cells resulted in an increased cell Ca^{2+} response to thrombin, which was evident at the peak but also in the prolonged phase of the response, persisting for some 16 min after stimulation. Although these authors concluded that polycystin-1 was regulating Ca^{2+} release from the ER, their data actually showed that removal of bath Ca^{2+} brought the prolonged phase responses of control and transgenic cells together and caused a much greater reduction in the peak response of the transgenic cells compared with the controls. Loss of functional polycystin-1 therefore appeared to result in a greater dependency on external Ca^{2+}, a finding very similar to our observations of the effect of the sIgPKD193 fusion protein. Therefore, the effects of the sIgPKD193 fusion protein described in the present study seem to indicate that the sIgPKD193 fusion protein acted as a dominant negative in the M1 cortical collecting duct cells, promoting increased store-operated Ca^{2+} entry through inhibition of the function of native polycystin-1.

The pathophysiological significance of our findings may be assessed in the context of what is known of disease mechanisms in ADPKD. In ADPKD, the epithelial cells lining the cysts are derived from proximal and distal tubules, both of which usually function to reabsorb fluid from the tubule lumen. Clearly, for cyst expansion, fluid must be secreted in the cyst lumen at a rate that exceeds the rate of fluid reabsorption. In all secretory epithelia, fluid secretion is stimulated by increased intracellular cAMP or elevated cell Ca^{2+}, acting on cystic fibrosis transmembrane conductance regulator (CFTR) or Ca^{2+}-activated Cl^- channels, respectively (16). Even in typically reabsorptive renal tubular epithelia grown in tissue culture, fluid secretion can be activated by these stimuli, and there is some evidence that such pathways also exist in vivo (15). However, the role of agonist-stimulated Cl^- secretion in ADPKD is uncertain, and studies of cyst epithelia have not revealed any upregulation of CFTR-mediated secretion compared with a variety of noncystic renal tubular epithelial cell lines (35). Our data suggest that polycystin pathways may be involved in the regulation of fluid secretion in response to purinergic stimulation. This is a biologically plausible hypothesis, since all the components for purinergic pathway activation are present in the cyst environment (32). Furthermore, there is increasing evidence that polycystin pathways are involved in the regulation of intracellular Ca^{2+} homeostasis, perhaps modulating the activity of transient receptor potential-type channels that are thought to mediate store-operated Ca^{2+} entry in eukaryotic cells (37, 40).

How does the activity of the sIgPKD193 fusion protein relate to the function of full-length polycystin-1? Many other investigators have studied the activity of the truncated cytoplasmic COOH-terminus of polycystin-1. In such studies, some of the effects of the truncated fusion protein suggested that it might act like polycystin-1: induction of in-gel tubulogenesis, binding and activation of $G\alpha_1$ (28, 29). Others have shown effects suggesting interruption of the actions of polycystin-1: stabilization of β-catenin (22), transformation of the cAMP growth phenotype from normal to polycystic (17, 36, 41), and augmentation of ATP-stimulated Cl^- secretion (19). In other studies, the relationship to polycystin-1 pathways cannot be inferred easily, for example, activation of the transcription factor activator protein-1 (2), stabilization of RGS7 (21), and induction of an oocyte cation conductance of uncertain origin (38). Perhaps the manifestations of expression of the isolated COOH-terminus of polycystin-1 depend on the activity of endogenous pathways and the cell system examined. In our studies, expression of the sIgPKD193 fusion protein promoted a secretory phenotype, as would be predicted in cystic epithelia. Thus, in our experimental system, it appears that the fusion protein might have interrupted the function of the native full-length polycystin-1 protein. This conclusion is strengthened by the data of Nauli et al. (27), which appears to support a role for polycystin-1 in downregulating agonist-stimulated Ca^{2+} entry.

Our observations are the first to directly indicate that polycystin-1 pathways regulate agonist-stimulated Ca^{2+} entry and provide, for the first time, a link between polycystin-1 and fluid secretion. Therefore, we propose that loss of functional polycystin-1 in ADPKD results in upregulation of store-operated Ca^{2+} entry after a Ca^{2+} release stimulus and that the subsequent activation of transepithelial Cl^- secretion may play an important role in cyst development and expansion.

We thank Ian Spencer, Ariel Wolff, and Xiaoyu Zhang for assistance.

DISCLOSURES

This work was funded by Satellite Research, The Polycystic Kidney Disease Foundation, and the National Kidney Foundation of Maryland. S. S. Wildman is a recipient of a Bogue International Travelling Fellowship. M. Sutters is a recipient of the Johns Hopkins Clinician Scientist award. S. S. Wildman and R. J. Unwin acknowledge the St. Peter's Trust (Les Clark Fund) for support.

REFERENCES

1. **Aguiari G, Campanella M, Manzati E, Pinton P, Banzi M, Moretti S, Piva R, Rizzuto R, and del Senno L.** Expression of polycystin-1 C-terminal fragment enhances the ATP-induced Ca^{2+} release in human kidney cells. *Biochem Biophys Res Commun* 301: 657–664, 2003.
2. **Arnould T, Kim E, Tsiokas L, Jochimsen F, Gruning W, Chang JD, and Walz G.** The polycystic kidney disease 1 gene product mediates protein kinase C alpha-dependent and c-Jun N-terminal kinase-dependent activation of the transcription factor AP-1. *J Biol Chem* 273: 6013–6018, 1998.
3. **Bailey MA, Imbert-Teboul M, Turner C, Srai SK, Burnstock G, and Unwin RJ.** Evidence for basolateral P2Y6 receptors along the rat proximal tubule: functional and molecular characterization. *J Am Soc Nephrol* 12: 1640–1647, 2001.
4. **Barrett KE and Keely SJ.** Chloride secretion by the intestinal epithelium: molecular basis and regulatory aspects. *Annu Rev Physiol* 62: 535–572, 2000.
5. **Bidet M, De Renzis G, Martial S, Ruberra I, Tauc M, and Poujeol P.** Extracellular ATP increases $[Ca]_i$ in distal tubule cells. I. Evidence for a P2Y2 receptor. *Am J Physiol Renal Physiol* 279: F92–F101, 2000.
6. **Boese SH, Glanville M, Aziz O, Gray MA, and Simmons NL.** Ca^{2+} and cAMP-activated Cl^- conductances mediate Cl^- secretion in a mouse renal inner medullary collecting duct cell line. *J Physiol* 523: 325–338, 2000.
7. **Borle A, Borle C, Dobransky P, Gorecka-Tisera A, Bender C, and Swain K.** Effects of low extracellular Ca^{2+} on cytosolic free Ca^{2+}, Na^+, and pH of MDCK cells. *Am J Physiol Cell Physiol* 259: C19–C25, 1990.
8. **Carew MA, Yang X, Schultz C, and Shears SB.** Myo-inositol 3,4,5,6-tetrakisphosphate inhibits an apical calcium-activated chloride conductance in polarized monolayers of a cystic fibrosis cell line. *J Biol Chem* 275: 26906–26913, 2000.
9. **Cuffe JE, Bielfeld-Ackermann A, Thomas J, Leipziger J, and Korbmacher C.** ATP stimulates Cl^- secretion and reduces amiloride-sensitive Na^+ absorption in M-1 mouse cortical collecting duct cells. *J Physiol* 524: 77–90, 2000.
10. **Erb L, Lustig K, Sullivan D, Turner J, and Weisman G.** Functional expression and photoaffinity labeling of a cloned P2U purinergic receptor. *Proc Natl Acad Sci USA* 90: 10449–10453, 1993.
11. **European Polycystic Kidney Disease Consortium.** The polycystic kidney disease 1 gene encodes a 14 kb transcript, and lies within a duplicated region on chromosome 16. *Cell* 77: 881–894, 1994.
12. **Fan J and Palade P.** Perforated patch recording with beta-escin. *Pflügers Arch* 436: 1021–1023, 1998.
13. **Fick-Brosnahan G, Belz M, McFann K, Johnson A, and Schrier R.** Relationship between renal volume growth and renal function in autosomal dominant polycystic kidney disease: a longitudinal study. *Am J Kidney Dis* 39: 1127–1134, 2002.
14. **Gandhi R, Elble RC, Gruber AD, Schreur KD, Ji H-L, Fuller CM, and Pauli BU.** Molecular and functional characterization of a calcium-sensitive chloride channel from mouse lung. *J Biol Chem* 273: 32096–32101, 1998.
15. **Grantham JJ and Wallace DP.** Return of the secretory kidney. *Am J Physiol Renal Physiol* 282: F1–F9, 2002.
16. **Greger R.** The membrane transporters regulating epithelial NaCl secretion. *Pflügers Arch* 432: 579–588, 1996.
17. **Hanaoka K and Guggino W.** cAMP regulates cell proliferation and cyst formation in autosomal polycystic kidney disease cells. *J Am Soc Nephrol* 11: 1179–1187, 2000.
18. **Hirt R, Poulain-Godefroy O, Billotte J, Kraehenbuhl J, and Fasel N.** Highly inducible synthesis of heterologous proteins in epithelial cells carrying a glucocorticoid-responsive vector. *Gene* 111: 199–206, 1992.
19. **Hooper K, Unwin R, and Sutters M.** The isolated C-terminus of polycystin-1 promotes increased ATP-stimulated chloride secretion in a collecting duct cell line. *Clin Sci (Colch)* 104: 217–221, 2003.
20. **International Polycystic Kidney Disease Consortium.** Polycystic kidney disease: the complete structure of the PKD1 gene, and its protein. *Cell* 81: 89–98, 1995.
21. **Kim E, Arnould T, Sellin L, Benzing T, Comella N, Kocher O, Tsiokas L, Sukhatme VP, and Walz G.** Interaction between RGS7 and polycystin. *Proc Natl Acad Sci USA* 96: 6371–6376, 1999.
22. **Kim E, Arnould T, Sellin LK, Benzing T, Fan MJ, Gruning W, Sokol SY, Drummond I, and Walz G.** The polycystic kidney disease 1 gene product modulates Wnt signaling. *J Biol Chem* 274: 4947–4953, 1999.
23. **King BF and Burnstock G.** Understanding G protein-coupled receptors and their role in the CNS. In: *Purinergic Receptors*, edited by Davies CH. Philadelphia, PA: Oxford Univ. Press, 2002, chapt. 21, p. 422–439.
24. **Kuruma A and Hartzell HC.** Bimodal control of a Ca^{2+}-activated Cl^- channel by different Ca^{2+} signals. *J Gen Physiol* 115: 59–80, 1999.
25. **Lu W, Shen X, Pavlova A, Lakkis M, Ward CJ, Pritchard L, Harris PC, Genest DR, Perez-Atayde AR, and Zhou J.** Comparison of Pkd1-targeted mutants reveals that loss of polycystin-1 causes cystogenesis and bone defects. *Hum Mol Genet* 10: 2385–2396, 2001.
26. **Lustig K, Shiau A, Brake A, and Julius D.** Expression cloning of an ATP receptor from mouse neuroblastoma cells. *Proc Natl Acad Sci USA* 90: 5113–5117, 1993.
27. **Nauli S, Alenghat F, Y L, Williams E, Vassilev P, Li X, Elia A, Lu W, Brown E, Quinn S, Ingber D, and Zhou J.** Polycystins 1 and 2 mediate mechanosensation in the primary cilium of kidney cells. *Nat Genet* 33: 129–137, 2003.
28. **Nickel C, Benzing T, Sellin L, Gerke P, Karihaloo A, Liu Z-X, Cantley LG, and Walz G.** The polycystin-1 C-terminal fragment triggers branching morphogenesis and migration of tubular kidney epithelial cells. *J Clin Invest* 109: 481–489, 2002.
29. **Parnell SC, Magenheimer BS, Maser RL, Rankin CA, Smine A, Okamoto T, and Calvet JP.** The polycystic kidney disease-1 protein, polycystin-1, binds and activates heterotrimeric G-proteins in vitro. *Biochem Biophys Res Commun* 251: 625–631, 1998.
30. **Putney JW Jr, Broad LM, Braun F-J, Lievremont J-P, and Bird GSJ.** Mechanisms of capacitative calcium entry. *J Cell Sci* 114: 2223–2229, 2001.
31. **Rubera I, Tauc M, Bidet M, Verheecke-Mauze C, De Renzis G, Poujeol C, Cuiller B, and Poujeol P.** Extracellular ATP increases $[Ca^{2+}]_i$ in distal tubule cells. II. Activation of a Ca^{2+}-dependent Cl^- conductance. *Am J Physiol Renal Physiol* 279: F102–F111, 2000.
32. **Schwiebert EM, Wallace DP, Braunstein GM, King SR, Peti-Peterdi J, Hanaoka K, Guggino WB, Guay-Woodford LM, Bell PD, Sullivan LP, Grantham JJ, and Taylor AL.** Autocrine extracellular purinergic signaling in epithelial cells derived from polycystic kidneys. *Am J Physiol Renal Physiol* 282: F763–F775, 2002.
33. **Stoos BA, Naray-Fejes-Toth A, Carretero OA, Ito S, and Fejes-Toth G.** Characterization of a mouse cortical collecting duct cell line. *Kidney Int* 39: 1168–1175, 1991.
34. **Suarez-Huerta N, Pouillon V, Boeynaems J-M, and Robaye B.** Molecular cloning and characterization of the mouse P2Y4 nucleotide receptor. *Eur J Pharmacol* 416: 197–202, 2001.
35. **Sullivan LP, Wallace DP, and Grantham J.** Epithelial transport in polycystic kidney disease. *Physiol Rev* 78: 1165–1191, 1998.
36. **Sutters M, Yamaguchi T, Maser RL, Magenheimer BS, St. John PL, Abrahamson DR, Grantham JJ, and Calvet JP.** Polycystin-1 transforms the cAMP growth-responsive phenotype of M-1 cells. *Kidney Int* 60: 484–494, 2001.
37. **Tsiokas L, Arnould T, Zhu C, Kim E, Walz G, and Sukhatme VP.** Specific association of the gene product of PKD2

with the TRPC1 channel. *Proc Natl Acad Sci USA* 96: 3934–3939, 1999.
38. **Vandorpe DH, Chernova MN, Jiang L, Sellin LK, Wilhelm S, Stuart-Tilley AK, Walz G, and Alper SL.** The cytoplasmic C-terminal fragment of polycystin-1 regulates a Ca^{2+}-permeable cation channel. *J Biol Chem* 276: 4093–4101, 2001.
39. **Viana F, de Smedt H, Droogmans G, and Nilius B.** Calcium signaling through nucleotide receptor P2Y2 in cultured human vascular endothelium. *Cell Calcium* 24: 117–127, 1998.
40. **Xu X, Li H, Guggino W, and Montell C.** Coassembly of TRP and TRPL produces a distinct store-operated conductance. *Cell* 89: 1155–1164, 1997.
41. **Yamaguchi T, Pelling JC, Ramaswamy NT, Eppler JW, Wallace DP, Nagao S, Rome LA, Sullivan LP, and Grantham JJ.** cAMP stimulates the in vitro proliferation of renal cyst epithelial cells by activating the extracellular signal-regulated kinase pathway. *Kidney Int* 57: 1460–1471, 2000.